Cancer Management and Research

Elevate Series

Open Access Full Text Article

ORIGINAL RESEARCH

Circ_CIT Promotes Nasopharyngeal Carcinoma Progression and Macrophage M2 Polarization Through miR-409-3p/ZEB1 Axis

Chengxian Ma[1,2], Jie Chen[3], Chenjing Zhu[1], Jianlin Wang[4], Suning Huang[2], Xinbin Pan[2], Yang Liu[2], Yusi Xie[2], Ziyang Zhou[2], Xia He[1]

[1]Nanjing Medical University, Jiangsu Institute of Cancer Research, Nanjing, People's Republic of China; [2]Department of Radiation Oncology, Guangxi Medical University Cancer Hospital, Nanning, People's Republic of China; [3]Nanjing Jiang Ning Hospital, The Affiliated JiangNing Hospital of Nanjing Medical University, Nanjing, People's Republic of China; [4]Department of Radiotherapy, The Affiliated Changzhou Second People's Hospital of Nanjing Medical University, Changzhou, People's Republic of China

Correspondence: Xia He, Email hexiabm@163.com

Purpose: Circular RNAs (circRNAs) play a crucial role in the progression of various cancers, including nasopharyngeal carcinoma (NPC). However, the mechanism of circRNA in the progression of NPC remains to be elucidated.

Patients and Methods: The expression levels of circ_CIT, microRNA-409-3p and ZEB1 in NPC tissues were detected by Real-time quantitative PCR (qRT-PCR). Nuclear separation and fluorescence in situ hybridization (FISH) assays were used to determine the localization of circ_CIT. Dual luciferase reporter was performed to confirm the binding of circ_CIT with micro (miR)-409-3p. Cellular behaviors were determined using Cell Counting Kit-8 (CCK-8), colony formation, wound healing, transwell and macrophage chemotaxis assays. Enzyme Linked Immunosorbent Assay (ELISA) and immunofluorescence Assays was used to evaluated macrophage markers.

Results: We identified that circ_CIT was mainly located in the cytoplasm. Circ_CIT expression was increased in NPC tissues and cell lines. Knockdown of circ_CIT inhibited cell proliferation, invasion and migration. Circ_CIT-mediated NPC tumorigenesis by sponging miR-409-3p and promoting ZEB1 expression. The inhibitors of miR-409-3p could reverse the effects of circ_CIT knockdown on NPC cells. The expression of circ_CIT and ZEB1 was found to be positively correlated with NPC tumor stage. Downregulation of expression of circ_CIT could promote macrophage M2 polarization through NPC cells. Overexpression of ZEB1 could reverse the inhibitory effect of circ_CIT knockdown on the polarization of macrophages to M2 phenotype.

Conclusion: Highly expressed circ_CIT adsorbs miR-409-3p to upregulate ZEB1 expression, thereby promoting the proliferation and metastatic ability of NPC cells and activating macrophage M2 polarization. Therefore, circ_CIT may be a potential therapeutic target for NPC patients.

Keywords: circRNA, miR-409-3p, nasopharyngeal carcinoma, ZEB1, epithelial-mesenchymal transition, macrophage

Introduction

Nasopharyngeal carcinoma (NPC) derives from nasopharyngeal epithelium, presenting a high malignant behavior. Epidemiological trends in the past decade have shown that its incidence has declined gradually, and mortality has been reduced substantially.[1] This is mainly due to the advancements in imaging technology and the in-depth application of individualized comprehensive chemo-radiotherapy. However, the majority of NPC patients are diagnosed at stage III or IV, and 30% of NPC patients eventually develop distant metastases and/or recurrence after comprehensive chemo-radiotherapy.[2,3] Thus, it is important to clarify the molecular mechanism of local invasion and metastasis of NPC.

In recent years, a large number of non-coding RNA has been found to play important biological roles in tumors.[4–6] Especially, the discovery of circular RNA has further enriched the mechanism of post-transcriptional regulation.[7] The most exploratory function of circular RNAs (circRNAs) is to act as a master regulator of gene expression that perform to sequester or "sponge" other gene expression regulators, in particular microRNAs (miRNAs). They have also been shown to function by directly regulating transcription and interfering with splicing mechanisms.[8,9] Some scholars have

Received: 27 March 2025
Accepted: 29 July 2025
Published: 18 August 2025

confirmed that circRNA plays a crucial role in the occurrence and progression of a variety of human cancers including NPC.[10–12] For example, our research group found that circ-0046263 plays a tumor-promoting role in NPC to enhance malignant behavior through the miR-133a-5p/IGFBP3 axis.[12] However, the role of circRNA in the invasion and metastasis of NPC has not been fully elucidated. A large number of circRNAs whose effects are unknown need to be explored.

In the present research, we identified a novel circRNA, circ_CIT (has_circ_0028705), which is abnormally expressed in NPC tissues and may regulate the progression of NPC metastasis. Our experimental results showed that the expression of circ_CIT was upregulated in NPC tissue samples and positively correlated with disease stage. Experimental results showed that knocking down circ_CIT inhibited the proliferation, migration and invasion ability of NPC cells. Further mechanism studies found that circ_CIT could act as a molecular sponge to adsorb miR-409-3p and promote the progression of NPC and macrophage M2 polarization by up-regulating the expression of miR-409-3p's downstream target gene ZEB1. Therefore, our study clarified the regulatory mechanism of circ_CIT in NPC and provided a potential prognostic biomarker and therapeutic target for NPC.

Material and Methods

Patients and Samples

Eighty cases of frozen NPC tissue and forty normal nasopharyngeal epithelial tissues were collected from the Department of the Radiotherapy Center of Jiangsu Cancer Hospital (Nanjing, China). All tissue samples were confirmed by pathological examination. The clinical stages of all NPC patients were recorded according to the 8th edition of the American Joint Committee on Cancer Staging Manual. The study was approved by the Ethics Committee of Jiangsu Cancer Hospital (Ethics Approval Number: (2021)413). All participants in this study provided written informed consent, in accordance with the Declaration of Helsinki.

Cell Culture and Transfection

Human NPC cell lines (5–8F (high tumorigenesis, high metastasis and low differentiation), 6–10B (low tumorigenesis, low metastasis and low differentiation), SUNE1 (high metastasis and low differentiation), CNE1 (low metastasis and high differentiation), CNE2 (low metastasis and low differentiation) and C666-1 (high tumorigenesis, low metastasis and low differentiation)), the human monocytic leukemia cells (THP-1) and the normal nasopharynx epithelial cell line (NP69) were provided by the Laboratory of Radiotherapy, Jiangsu Cancer Hospital. THP-1, 5–8F, 6–10B, SUNE1, CNE1, CNE2 and C666-1 cells were cultured in RPMI 1640 (Corning, Corning, New York, USA) supplemented with 10% fetal bovine serum (FBS; Gibco, Grand Island, NY, USA) while NP69 cells were cultured in serum-free medium Keratinocyte-SFM (Gibco) at 37°C under 5% CO_2 condition. Phorbol-12-myristate-13-acetate (10 ng/mL, PMA, Sigma, St. Louis, MO, USA) was added into the RPMI 1640 medium for 24 h to promote the differentiation of THP-1. This type of cell was treated as M0 macrophage (M0 group) in the present study. Additionally, the cell lines we used were authenticated by STR profile. Small interfering RNA (siRNA) targeting circ_CIT, ZEB1, negative control (si-NC), miR-409-3p mimics, NC mimics, miR-409-3p inhibitor, NC inhibitor, oe-ZEB1 lentivirus and oe-NC were manufactured by Gene-Pharma (Shanghai, China). NPC cells were transfected using L lipofectamine-2000 (Invitrogen, Carlsbad, CA, USA) in accordance with the manufacturer's instructions.

Polarization Assay of Macrophages

Different groups of 5–8F and 6–10B cells were seeded in a 6-well plate (1×10^6 cells). The supernatant of cells was collected. M0 Macrophages were seeded at 1×10^6 cells in 6-well plates in tumor conditioned medium (medium containing 5–8F and 6–10B cell supernatant) and were incubated for 48 h. The expression levels of the M1 (Interleukin-6 (IL-6), Tumor Necrosis Factor-α (TNF-α) and Differentiation 80 (CD80)) macrophage markers and M2 (CD206, CD163 and IL-10) macrophage markers were determined to study the effects of NPC cell supernatant on polarization of macrophage.

Reverse Transcription-Polymerase Chain Reaction (RT-PCR)

Total RNA was extracted using TRIzol reagent (Invitrogen) and RNA integrity was assessed on a 1% agarose/formaldehyde gel. The cDNA was obtained from 1 μg of total RNA using the SuperScript II First-Strand cDNA Synthesis Kit (Invitrogen) in a final volume of 20 μL. cDNA was amplified by PCR using 1 μL per sample primers. Thermal cycling conditions: 95°C for 2 min, 95°C for 30s 35 cycles, 52°C-60°C (depending on the Tm of each set of primers) for 1 min, 72°C for 30s. GAPDH was amplified as an internal control. Finally, RT-PCR products were separated by 2% agarose gel electrophoresis, stained with ethidium bromide, and then photographed under a UV illuminator (Thermo Fisher Scientific, Waltham, MA, USA).

RNA Extraction and Quantitative Real-Time Polymerase Chain Reaction (qRT-PCR)

Total RNA was obtained using TRIzol (Invitrogen) based on the user's manual. Genomic DNA (gDNA) in the cell was extracted with mammalian genomic DNA extraction kit (Beyotime, Shanghai, China). QRT-PCR was carried out using SYBR Green PCR Master Mix (Takara, Shanghai, China) on a 7500 FAST real-time PCR machine (Applied Biosystems, Thermo Fisher Scientific). Gene expression was normalized against U6 or GAPDH. The relative level of each RNA was calculated using the Ct ($2^{-\Delta\Delta CT}$) method. The sequences used in qPCR are as follows: GAPDH forward 5′-GGAGCGAGATCCCTCCAAAAT-3′; GAPDH reverse 5′-GGCTGTTGTCATACTTCTCATGG-3′; U6 forward 5′-CTCGCTTCGGCAGCACA-3′; U6 reverse 5′-AACGCTTCACGAATTTGCGT-3′; circ_CIT forward 5′-AAGGTCTTTGCTGCCATCCT-3′; circ_CIT reverse 5′-CGGGCTTGTGCTTCGAGATA-3′; CIT forward 5′-ATATGGAGCGCGGAATCCTTT-3′, CIT reverse 5′-TCAGCTATGGTGTCGGAATACT-3′, miR-409-3p forward 5′-GCCGAGGAATGTTGCTCGGT-3′, miR-409-3p reverse 5′-GTGCAGGGTCCGAGGT-3′; ZEB1 forward 5′-TCAAAAGGAAGTCAATGGACAA-3′, ZEB1 reverse 5′-TCTGTAACACTTTCTTCTTCCA-3′; IL-6 forward 5′-TTCGGTCCAGTTGCCTTCTC-3′; IL-6 reverse 5′-GAGGTGAGTGGCTGTCTGTG-3′; TNF-α forward 5′-CCCTCACACTCAGATCATCTTCT-3′; TNF-α reverse 5′-GCTACGACGTGGGCTACAG-3′; CD80 forward 5′-TCTCAGAAGTGGAGTCTTACCCT-3′; CD80 reverse 5′-GATTGGAGGGTGTTCCTGGG-3′; CD206 forward 5′-CCAAACGCCTTCATTTGCCA-3′; CD206 reverse 5′-ACCTTCCTTGCACCCTGATG-3′; CD163 forward 5′-CCGGGAGATGAATTCTTGCCT-3′; CD163 reverse 5′-GGTATCTTAAAGGCTCACTGGGT-3′; IL-10 forward 5′-AGGGCACCCAGTCTGAGAAC-3′; IL-10 reverse 5′-TCTTCACTCTGCTGAAGGCAT-3′.

Western Blot Analysis

Cells were harvested and homogenized in the lysis buffer and their concentrations were determined by a bicinchoninic acid (BCA) protein assay kit (Beyotime). Proteins were separated by electrophoresis and transferred into polyvinylidene difluoride (PVDF) membrane. Immunoblotting of membrane with the primary antibodies (ZEB1, 1:1000 dilutions; GAPDH 1:2000 dilutions). All the antibodies were purchased from Cell signaling Technology (Danvers, MA, USA). Finally, the image of the protein band was captured by the Tanon detection system using the enhanced electrochemiluminescence (ECL) reagent (Millipore, Billerica, MA, USA).

Subcellular Fractionation Location

The localization of circ_CIT in 5–8F and 6–10B cells was determined by subcellular fractionation assays. Nuclear and cytoplasmic RNA fractionations were performed using PARIS kit (Invitrogen) following the manufacturer's instruction, analyzed by RT-qPCR successively. GAPDH was an endogenous control for cytoplasm, whereas U6 was that for the nucleus.[13] Circ_CIT, GAPDH, and U6 expression levels in cytoplasmic and nuclear fractions of 5–8F and 6–10B cells were detected by RT-qPCR.

Fluorescence in situ Hybridization (FISH)

Fluorescence in situ hybridization (FISH) analysis was used to verify the position and expression of circ_CIT in NPC cells (5–8F, 6–10B) using a FISH kit (RiboBio, Guangzhou, China) according to the manufacturer's protocol. FISH is a molecular method that uses short DNA fragments (oligonucleotides) that are labelled with a fluorescent marker to target

specific groups of organisms.[14] Image J software (Version 1.8.0, National Institutes of Health) was used to circle the nuclear and cytoplasmic area and to analyzed the mean fluorescence intensity.

Colony Formation and Cell Viability Assay

The proliferation rate of 5–8F and 6–10B cells was detected using a Cell Counting Kit-8 (CCK-8) assay kit (Promega, Madison, Wisconsin, USA). 3000 cells per well were inoculated into 96-well plates, and 10 μL of CCK-8 solution was added to the cultured cells at a single time point. After incubation at 37°C for 1 h, each well was examined with a spectrophotometer at 450 nm. In the colony formation assay, after transfection, 1000 cells were spread in six well plates and incubated at 37°C for 10 days. The colonies were fixed with methanol, and then stained for 30 minutes using the Giemsa staining method. The colonies were observed and counted using Image J (version 1.8.0, National Institutes of Health).

Wound Healing Assay

5–8F and 6–10B cells were seeded in 6-well plates and cultured until full confluence. A straight wound was induced by scratching with a sterile pipette tip, and washed twice with phosphate-buffered saline (PBS). Cell migration was measured at 100× magnification under light microscopy at 0, 24 and 48 h.

Transwell Assay

Transwell assays were performed to evaluate the invasion of NPC cells. 5–8F and 6–10B cells were collected and plated into the upper chamber, which was pre-coated with Matrigel Matrix (BD Biosciences, Bedford, Ohio, USA), while 500 μL DMEM with 20% FBS was added to the lower compartment. After culture for 36 h, cells that had invaded across the membrane were fixed, stained and counted under a microscope.

Luciferase Reporter Assay

The wild type and mutant sequence in binding sites of circ_CIT and ZEB1 were cloned into the luciferase pcDNA3.1 vector (Promega). 5–8F and 6–10B cells were co-transfected using miR-409-3p mimics and circ_CIT/ZEB1 wild-type (Wt) or mutant (Mut) luciferase plasmids. After 48 hours, luciferase density was assessed using the Dual Luciferase Assay Kit (Promega) according to the Kit instructions.

Immunofluorescence Assay

Macrophages were fixed via 4% paraformaldehyde (Sigma) for 20 min and 0.5% Triton X-100 (Sigma) at room temperature for 15 min. Primary antibody CD206 (1: 50 dilutions, rabbit monoclonal, Abcam, Cambridge, UK) incubated cells at 4°C overnight. Then, the samples were cleaned and treated with Alexa Fluor-647-conjugated anti-rabbit IgG antibody (Abcam) for 1 h. After 4,6-diamino-2-phenyl indole (DAPI, Sigma) stained the samples, visualization was performed under a fluorescence microscope (BX53; Olympus, Tokyo, Japan).

Enzyme Linked Immunosorbent Assay (ELISA)

ELISA Kit of IL-10 was obtained from R&D Systems (Minneapolis, MN, USA) and ELISA Kit of TNF-α was obtained from Abcam according to manufacturer instructions. Briefly, the cell culture supernatant was collected, centrifuged at 1,000 g at 4°C for 30 min, and the supernatant was stored at −80°C until use. The samples to be tested were thawed on ice. Standard wells were set up, and then 50 μL of pre-replaced standards at different concentrations were added to each well. Next, 50 μL of each sample to be tested was added to each well. Thereupon, 50 μL of horseradish was added per well and incubated for 1 h at 37°C. The liquid was later discarded, and 300 μL of cleaning solution was added. After 2 min, the cleaning solution was discarded, and the microwell plate was patted dry on the absorbent paper to remove any residual liquid. The microwell plate was rinsed another 5 times, and then 50 μL of the substrate was added to each well and incubated for 15 min. Lastly, 50 μL of a stop solution (2 mol/L H_2SO_4) was added to terminate the reaction, and the absorbance of each well was assessed at a wavelength of 450 nm using a spectrophotometer (Thermo Fisher Scientific).

Macrophage Chemotaxis Assay

PMA-induced THP-1 cells (M0 macrophages) were incubated with IL-4 and IL-13 (20 ng/mL IL-4 and IL-13; R&D Systems) for 48 h at 37°C to obtain M2 macrophages. The supernatant of 5–8F and 6–10B cells (400 μL) was added to the lower compartment of Transwell inserts. M2 macrophages (4×10^4 cells/well) were then overlaid onto the upper chamber. After 16 h at 37°C, the migrated cells were counted using a hemocytometer (Sigma).

Statistical Analysis

All statistical analyses were performed using SPSS software GraphPad Prism software (GraphPad Software Inc., La Jolla, CA). All experiments were performed at least three times independently. Data are presented as mean ± SD. Unpaired Student's *t*-test was used to compare two groups. One-way ANOVA was used in statistical studies involving multiple group comparisons, and Tukey's post hoc test was then applied. $P < 0.05$, Statistical significance was established.

Results

Validation of Circ_CIT

In the preliminary experiment, our research group found circ_CIT (has_circ_0028705), which is back-spliced of five exons (exons 5, 6, 7, 8 and 9) of CIT gene (chr12:120,260,623–120,288,079), located at q24, 23 (Figure 1A). In order to

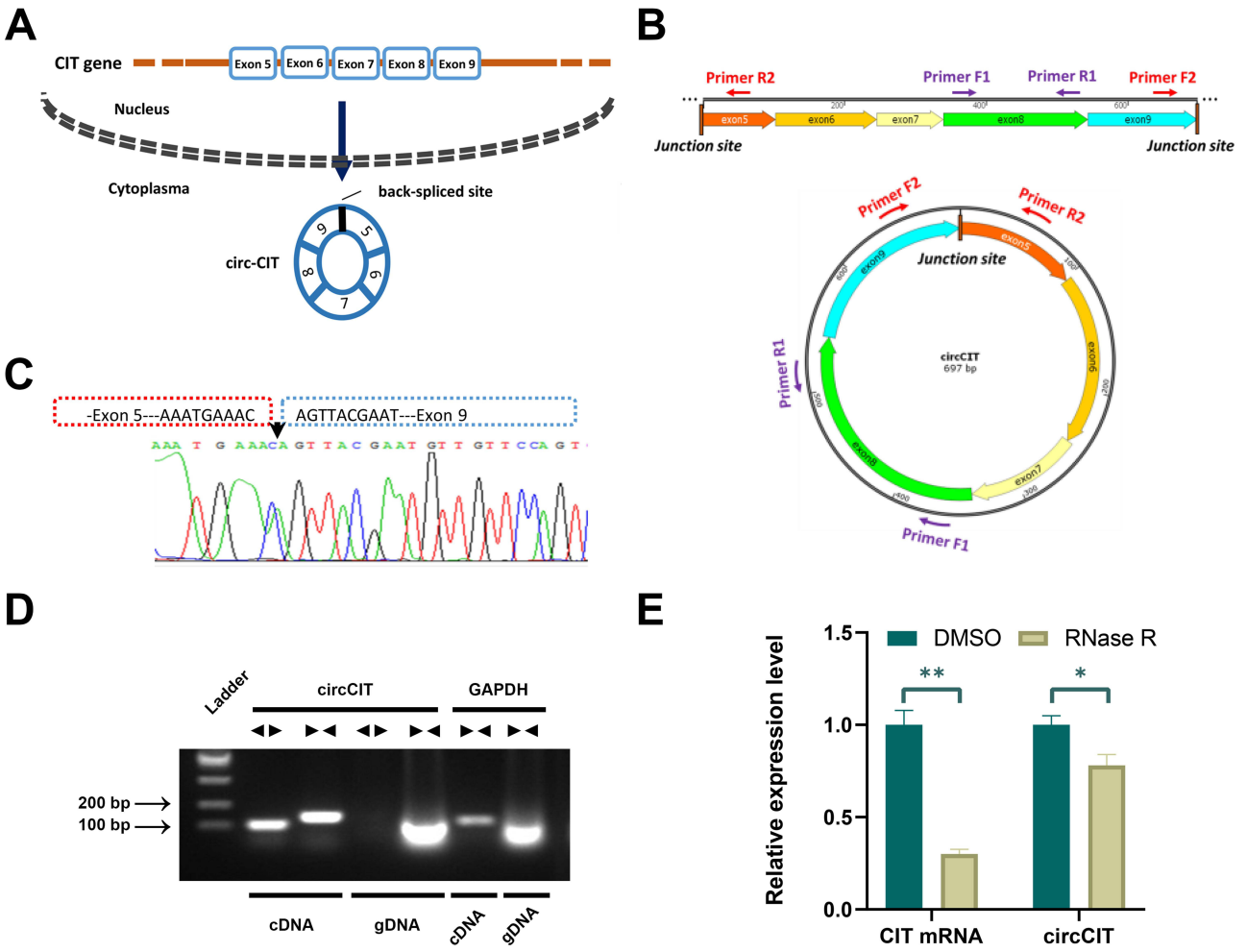

Figure 1 Validation of circ_CIT. (**A**) Schematic illustration demonstrates the formation of circ_CIT via the circularization of exons 5 to 9 in CIT. (**B**) The formation of circ_CIT. The head-to-tail splicing site of circ_CIT is indicated. (**C**) The presence of circ_CIT was validated by RT-PCR, followed by Sanger sequencing. (**D**) PCR validated the circularization of circ_CIT. Circ_CIT was amplified by divergent primers in cDNA but not gDNA. GAPDH was used as the negative control. (**E**) The RNase digestion experiment proved that circ_CIT is circular. The expression of circ_CIT or CIT mRNA was detected by qRT-PCR in the presence or absence of RNase R (n=3). * $P < 0.05$, ** $P < 0.01$.

https://doi.org/10.2147/CMAR.S526022

further characterize circ_CIT, we designed two sets of primers: divergent primers were used to amplify circular transcripts and convergent primers were used to detect linear transcripts (Figure 1B). We performed Sanger sequencing on the circular transcripts amplified by the divergent primers and confirmed their head-to-tail splicing (Figure 1C). However, either trans-splicing or genome rearrangements can produce this head-to-tail splicing pattern. Therefore, we used these two primers to amplify circular and linear transcripts of CIT in cDNA and gDNA. The results indicated that the divergent primer could amplify products in cDNA but not in gDNA (Figure 1D). In order to confirm the stability of circ_CIT, RNase R was used in the experiment. As shown in Figure 1E, CIT mRNA levels dropped sharply ($P < 0.01$), but circ_CIT was able to tolerate RNase R digestion ($P < 0.05$). Indeed, these data confirmed the existence of circ_CIT.

Circ_CIT Expression in NPC Cells

The expression of circ_CIT was detected in NPC cell lines using qRT-PCR (Figure 2A). As the results show, circ_CIT was up-regulated in NPC cell lines, especially in 5–8F and 6–10B (all $P < 0.01$). Therefore, we selected these two cell lines for further research. Next, we tested the location of circ_CIT. First, the nuclear and cytoplasmic separation experiment showed that circ_CIT was mainly located in the cytoplasm (Figure 2B). Furthermore, RNA FISH results also indicated that circ_CIT was mainly located in the cytoplasm (Figure 2C, all $P < 0.05$).

Decreased Expression Level of circ_CIT Suppress Proliferation, Migration and Invasion of NPC Cells

In order to explore the biological functions of circ_CIT in vitro, we designed two siRNAs and verified the knockdown efficiency (Figure 3A, all $P < 0.01$). After transfection of siRNA, the expression of circ_CIT was significantly down-regulated, while the mRNA level of CIT did not change significantly (Figure 3B). Then, we used clone formation

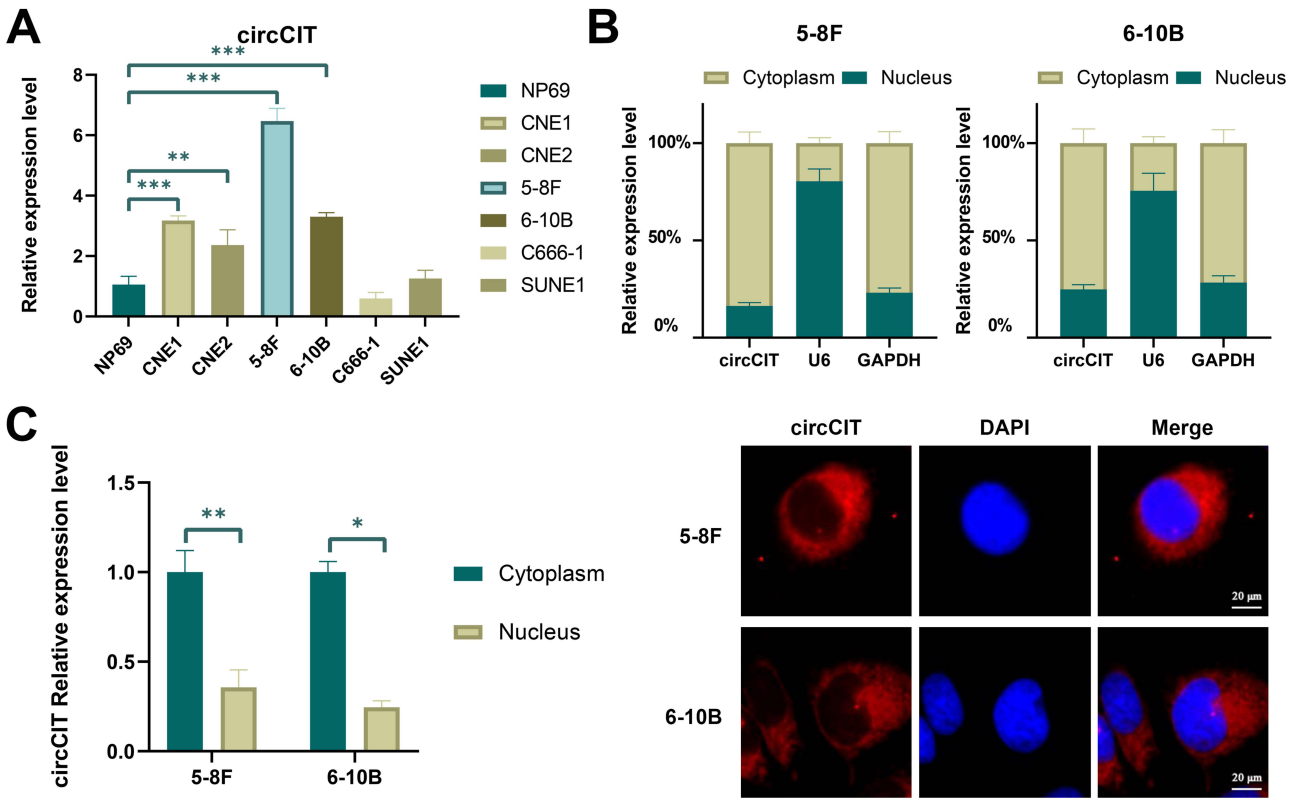

Figure 2 Circ_CIT expression in NPC cells. (**A**) Circ_CIT expression was detected by qRT-PCR in several human NPC cell lines (CNE1, CNE2, 5–8F, 6–10B, C666-1 and SUNE1) and normal nasopharyngeal epithelium cells (NP69); circ_CIT expression level was higher in NPC cells than in NP69. (**B**) Separation of nuclear and cytoplasmic fractions shown subcellular localization of circ_CIT. (**C**) FISH experiment showed that circ_CIT was mainly localized in the cytoplasm. Nuclei were stained with DAPI (blue), and circ_CIT probes were labeled with Alexa Fluor 593 (red); scale bars, 20 μm. All n=3. * $P < 0.05$, ** $P < 0.01$, ** $P < 0.001$.

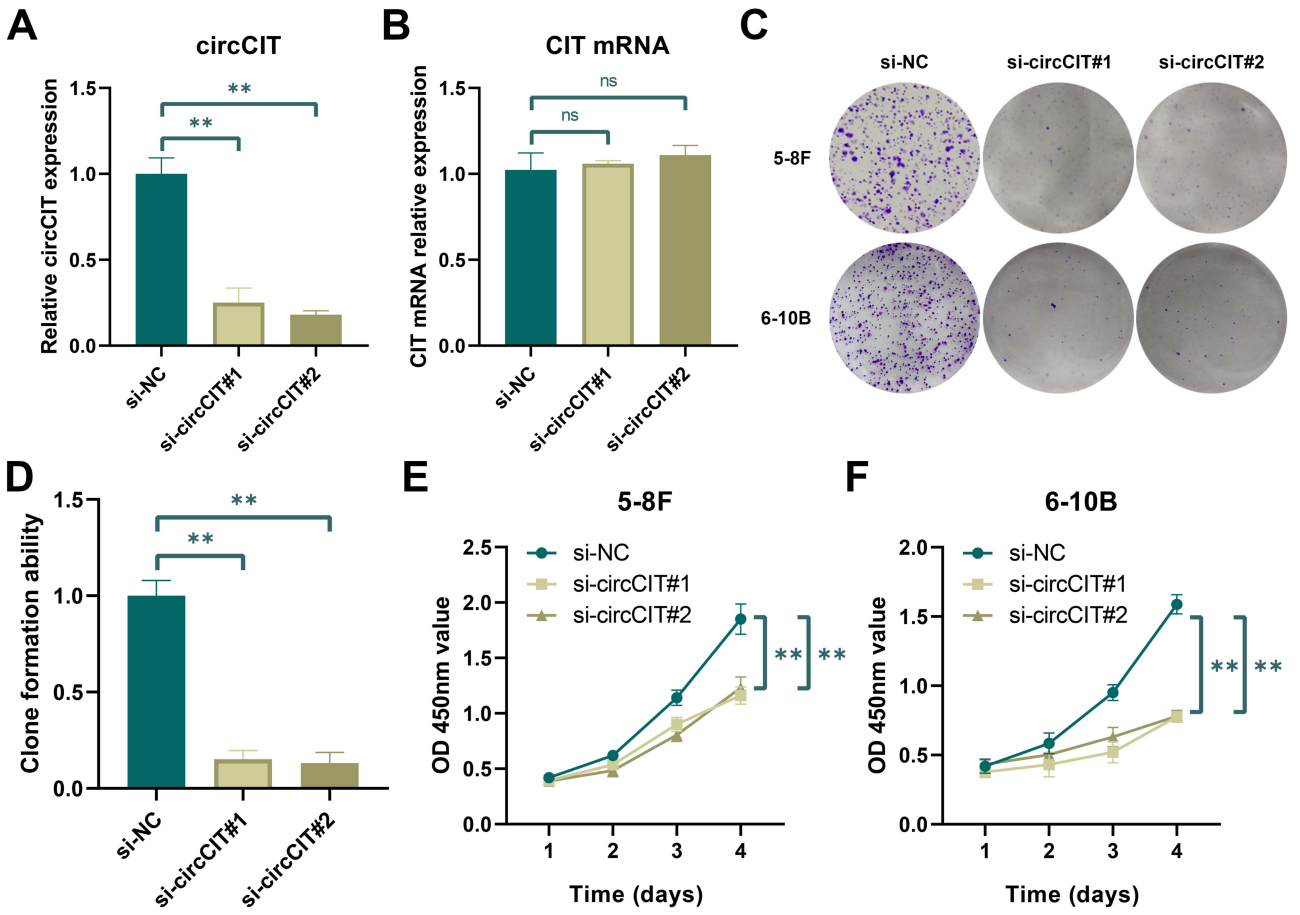

Figure 3 Decreased expression level of circ_CIT suppress proliferation of NPC cells. (**A**) The expression level of circ_CIT after knocking down circ_CIT with siRNA. (**B**) The expression level of CIT mRNA after knocking down circ_CIT. (**C**) The proliferative capacity of 5–8F and 6–10B cells were determined via colony-formation assay after knocking down circ_CIT. (**D**) Quantitative result of Figure C. (**E** and **F**) The proliferative capacity of 5–8F (**E**) and 6–10B (**F**) cells were determined via CCK8 assay after knocking down circ_CIT. All n=3. ** $P < 0.01$.

experiments and CCK-8 experiments to investigate the effect of circ_CIT on the proliferation of NPC cells. After transfection of siRNA in 5–8F and 6–10B, the results showed that knocking down circ_CIT significantly inhibited the proliferation of NPC cells (Figure 3C–F, all $P < 0.01$). To investigate the effect of circ_CIT on cell migration and invasion, wound healing and transwell assays were conducted on NPC cells. The results showed that knocking down circ_CIT significantly inhibited the migration and invasion ability of NPC cells (Figure 4A and B, all $P < 0.01$). In the wound healing experiment, we took pictures at 24 hours and 48 hours and measured the migration distance. The results showed that knocking down circ_CIT significantly inhibited the wound healing ability of NPC cells (Figure 4C and D, all $P < 0.01$).

Circ_CIT Targets miR-409-3p in NPC Cells

The previous results showed that circ_CIT was mainly located in the cytoplasm, and this circular RNA was more likely to act as a sponge of miRNA. Therefore, we used online software TargetScan to predict the miRNA that circ_CIT might adsorb (Figure 5A). We selected miRNAs with a comprehensive score of 90 or more for further research, and co-transfected the wild-type luciferase vector of circ_CIT and the mimics of miRNAs. The results showed that the luciferase activity was inhibited only after miR-409-3p mimics was transfected (Figure 5B, $P < 0.01$). We continued to use public databases to analyze the precursor sequence of miR-409-3p (Figure 5C) and the site where circ_CIT binds to it (Figure 5D). Wild-type and mutant circ_CIT were constructed for the dual luciferase reporter assay. MiR-409-3p

https://doi.org/10.2147/CMAR.S526022

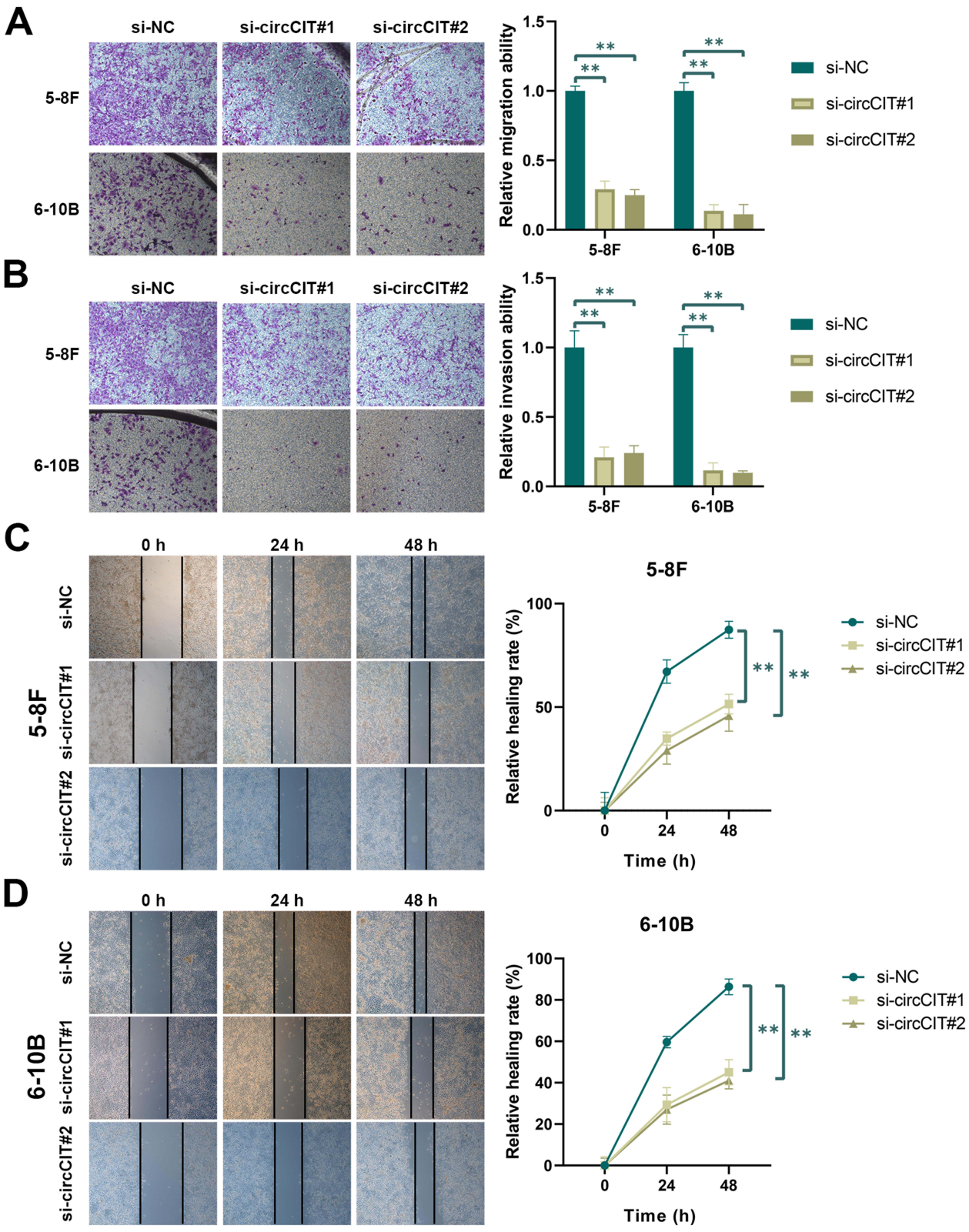

Figure 4 Circ_CIT affects the migration and invasion ability of NPC cells. (**A** and **B**) Transwell migration (**A**) and Matrigel invasion (**B**) assays were used to detect the migration and invasion capacity of NPC cells transfected with si-circ_CIT or si-NC. (**C** and **D**) Wound-healing assay was conducted to show that circ_CIT knockdown suppressed 5–8F (**C**) and 6–10B (**D**) cells migration ability. All n=3. ** $P < 0.01$.

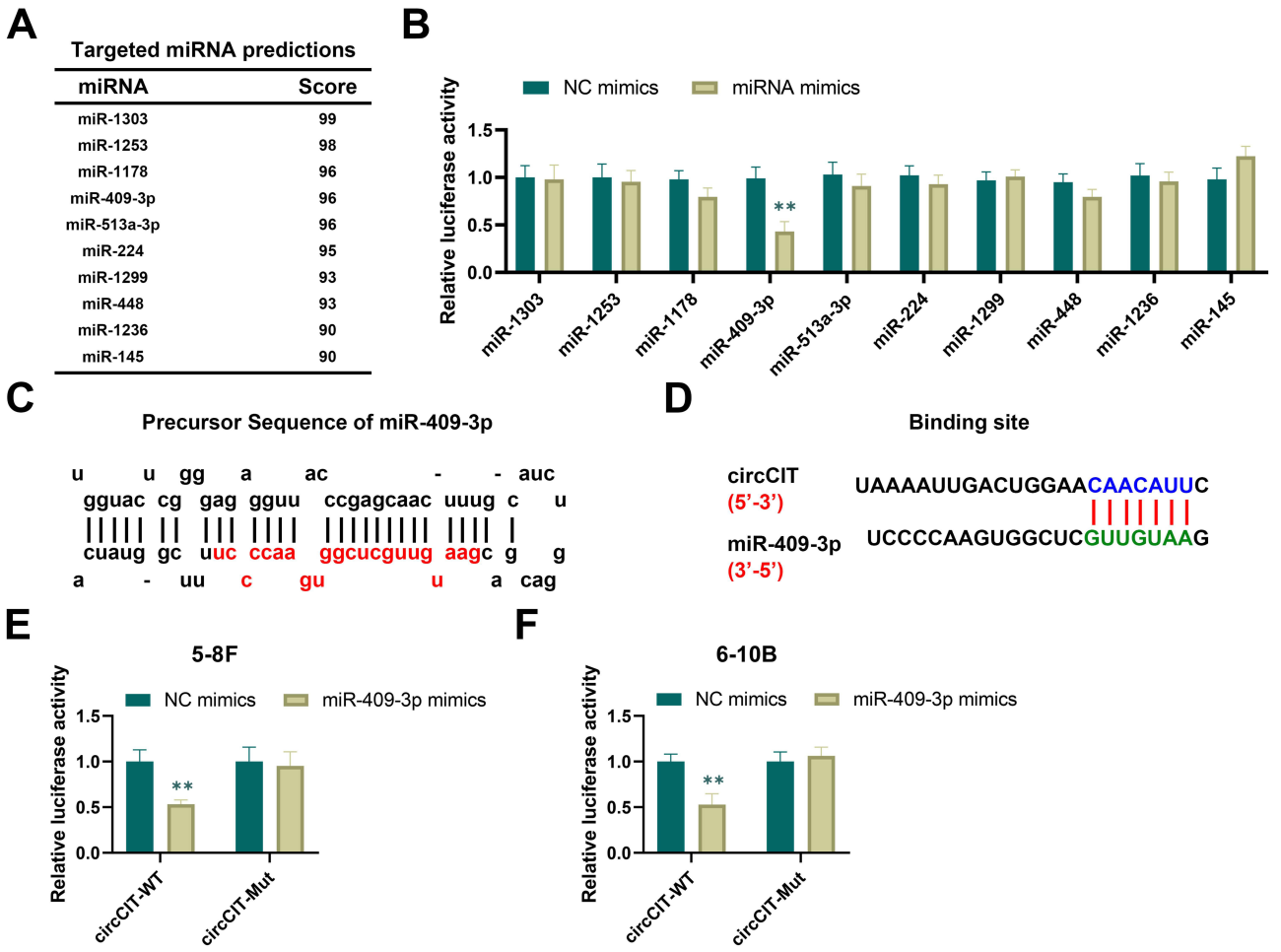

Figure 5 Circ_CIT targets miR-409-3p in NPC cells. (**A**) The ten highest-scoring target miRNAs of circ_CIT predicted by TargetScan. (**B**) The luciferase activity of circ_CIT in NPC cell line 5–8F after co-transfection with predicted target miRNAs. (**C**) Schematic diagram showing the precursor sequence of miR-409-3p. (**D**) A schematic drawing showing the putative binding sites of miR-409-3p with circ_CIT. (**E** and **F**) Dual luciferase reporter assays showed miR-409-3p directly bind to the circ_CIT and inhibit its luciferase activity in 5–8F cells (**E**) and 6–10B cells (**F**). All n=3. ** $P < 0.01$.

significantly reduced luciferase activity of cells transfected with circ_CIT-WT, but not circ_CIT-MUT (Figure 5E and F, all $P < 0.01$). The dual luciferase reporter assay indicated that Circ_CIT directly targets miR-409-3p in NPC cells.

MiR-409-3p Negatively Regulates the Migration, Invasion and Proliferation of NPC Cells

In order to evaluate the biological function of miR-409-3p in NPC cells, we transfected miR-409-3p mimics in 5–8F and 6–10B cells. The transfection efficiency showed that the expression level of miR-409-3p increased significantly after transfection of mimics (Figure 6A, all $P < 0.01$). The result of the clone formation experiment showed that the clone formation ability of mimics transfected cells was significantly reduced (Figure 6B, all $P < 0.01$). Compared with the control group, the wound healing ability of the cells transfected with mimics was significantly weakened (Figure 6C, all $P < 0.01$). In the transwell experiment, the number of cells that migrated and invaded in the experimental group was also significantly reduced (Figure 6D and E, all $P < 0.01$). The CCK-8 experiment showed that the cell viability was significantly reduced after transfection of mimics (Figure 6F, all $P < 0.01$). These results indicated that overexpression of miR-409-3p could inhibit the proliferation, invasion and migration of NPC cells in vitro. In addition, after knocking down miR-409-3p in NPC cells, we observed the opposite result (Figure S1, all $P < 0.01$).

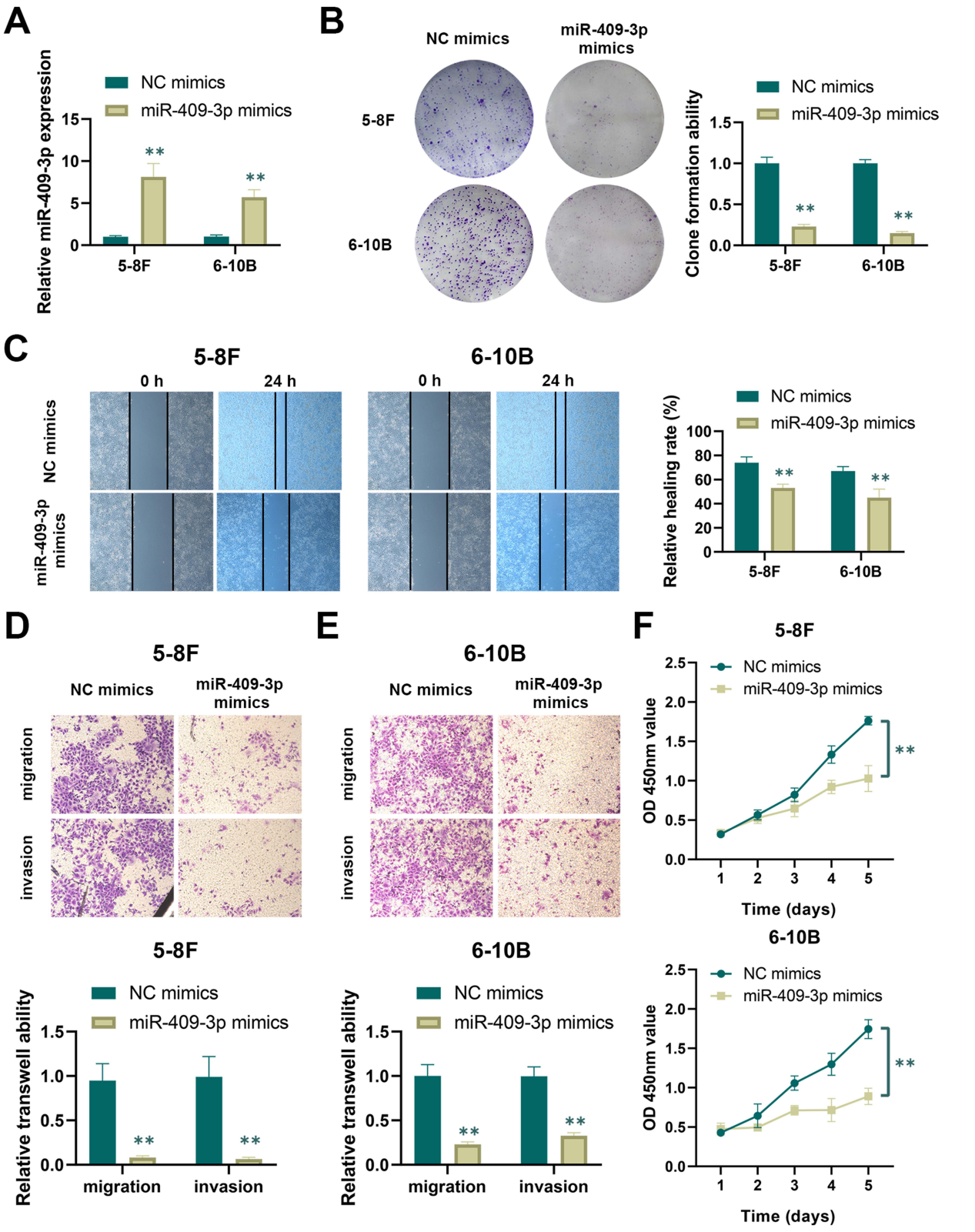

Figure 6 MiR-409-3p negatively regulates the migration, invasion and proliferation of NPC cells. (**A**) qRT-PCR show that miRNA mimics significantly increase the expression level of miR-409-3p. (**B**) Proliferation ability of miR-409-3p mimics transfected NPC cell line 5–8F and 6–10B was assessed by clone formation assay. (**C**) Wound-healing assay was conducted to show that miR-409-3p mimics suppressed cell migration ability. (**D** and **E**) Transwell migration and Matrigel invasion assays were used to detect the migration and invasion capacity of 5–8F (**D**) and 6–10B (**E**) NPC cells transfected with miR-409-3p mimics. (**F**) The proliferative capacity of NPC cells was determined via CCK-8 assay after transfected with miR-409-3p mimics. All n=3. ** $P < 0.01$.

Circ_CIT Promoted NPC Progression via the circ_CIT-miR-409-3p-ZEB1 Axis

To investigate whether circ_CIT enhanced the proliferation, migration, and invasion of NPC cells by interacting with miR-409-3p, we performed rescue experiments and co-transfected with si-circ_CIT and miR-409-3p inhibitor in 6–10B and 5–8F cells. CCK-8 assays (Figure 7A, all $P < 0.01$) and colony formation assays (Figure 7B, all $P < 0.01$) indicated that the circ_CIT expression inhibition significantly decreased proliferation ability, while silencing of miR-409-3p increased the proliferation ability on the base of knockdown of circ_CIT. Wound healing (Figure 7C, all $P < 0.01$) and Transwell assays (Figure 7D, all $P < 0.01$) results indicated that miR-409-3p downregulation could restore cell invasion and migration in NPC cells. Previous research pointed out that ZEB1 was confirmed as a direct target of miR-409-3p and inhibited ZEB1 expression by directly binding to the 3′ UTR.[15] We performed verification in NPC cells. We used public databases to analyze the site where ZEB1 binds to miR-409-3p (Figure S2A). Wild-type and mutant ZEB1 were constructed for the dual luciferase reporter assay. MiR-409-3p significantly reduced luciferase activity of cells transfected with ZEB1-WT, but not ZEB1-MUT (Figure S2B, $P < 0.01$). Western blot results showed that after

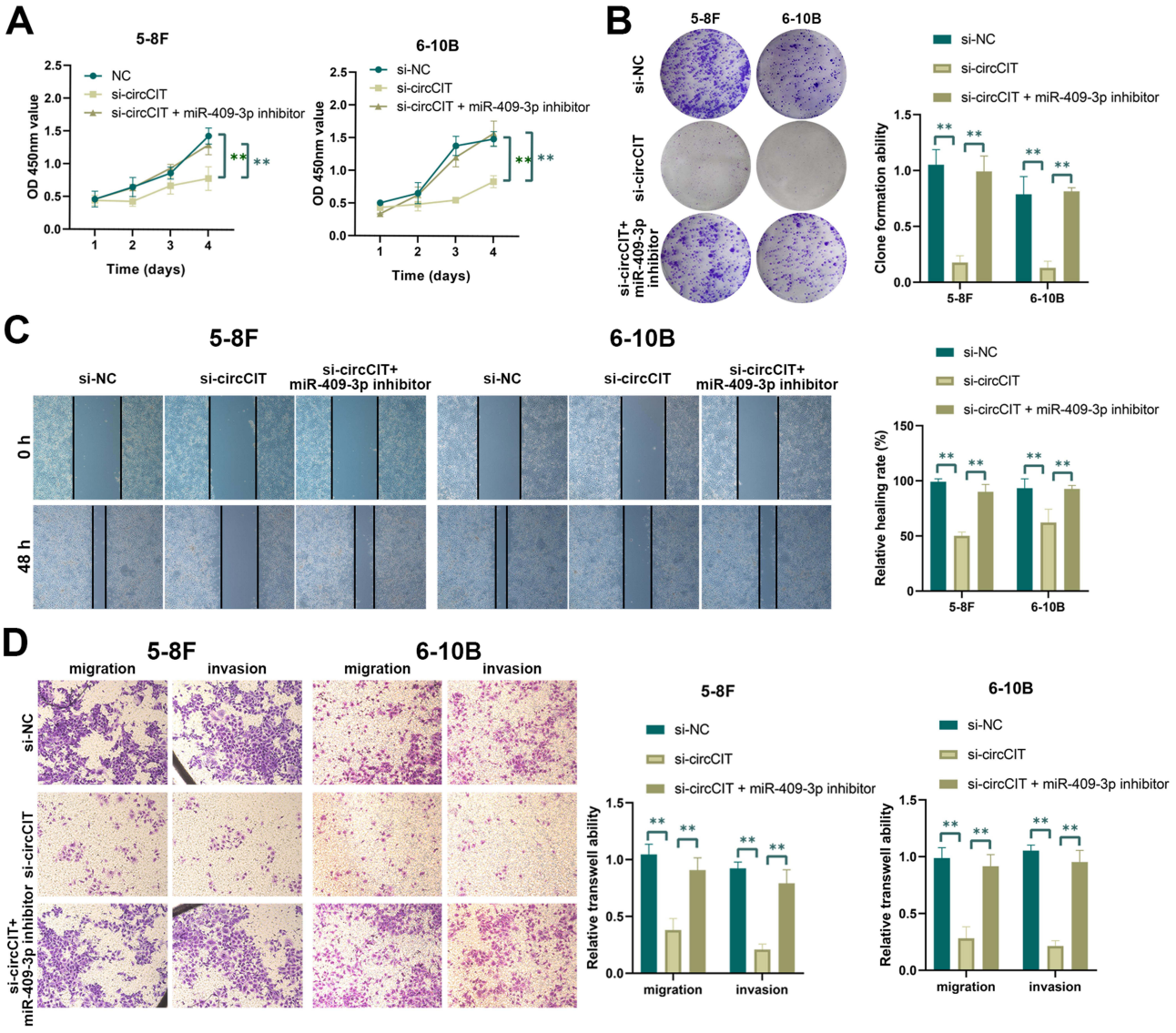

Figure 7 miR-409-3p inhibitor abolished the inhibiting effects of si-circ_CIT mimics on cell growth, migration and invasion. (**A**) miR-409-3p inhibitor can partially abolished the effects of inhibiting circ_CIT on NPC cell growth, as shown by CCK-8 assay. (**B**) miR-409-3p inhibitor can partially abolished the effects of inhibiting circ_CIT on cell proliferation, revealed by clone formation assay. (**C**) miR-409-3p inhibitor can partially abolished the effects of inhibiting circ_CIT on cell migration, revealed by wound-healing assay. (**D**) miR-409-3p inhibitor abolished the effects of inhibiting circ_CIT on cell migration and invasion. All n=3. ** $P < 0.01$.

https://doi.org/10.2147/CMAR.S526022

transfection with si-circ_CIT, the expression of ZEB1 was significantly down-regulated, while transfection with miR-409-3p inhibitor, the result was the opposite (Figure S2C, $P < 0.01$). Taken together, these findings indicated that circ_CIT primarily promoted the progression of NPC cells by targeting ZEB1.

Circ_CIT Is Up-Regulated in NPC Patient and Positively Correlates with Disease Stage

In order to verify the clinical significance of circ_CIT in NPC, we analyzed the correlation between the expression of circ_CIT in NPC and clinical staging data. The expression levels of circ_CIT, miR-409-3p, and ZEB1 were detected in the tumor tissues of 80 NPC tissues and 40 normal tissues (Figure S3A–C, all $P < 0.05$). The results showed that the expression level of circ_CIT and ZEB1 in tumor tissues was significantly higher than that in normal tissues, while the expression level of miR-409-3p was lower. This indicates that circ_CIT with the stable expression in the patients can be used as a biomarker of NPC. In addition, the expression of circ_CIT and ZEB1 was also found to be positively correlated with tumor stage, while the expression level of miR-409-3p was uncorrelated with stage (Figure S3D–F). Further analysis of the expression level of circ_CIT and ZEB1 in tumor tissues revealed that there was a positive weak correlation between them (Figure S3G, $P < 0.001$). The correlation analysis was performed to explore the relationships between circ_CIT and miR-409-3p, miR-409-3p and ZEB1 expression in NPC tissues. Results showed that there is no significant correlation between the expression levels of circ_CIT and miR-409-3p, as well as miR-409-3p and ZEB1 (Figure S3H and I).

Circ_CIT Regulates M2 Macrophage Polarization to NPC Cells Through ZEB1

Previous studies have shown that ZEB1 is regulated by non-coding RNA to regulate the polarization and infiltration of macrophages.[16] In order to verify whether circ_CIT mediates ZEB1 regulation of macrophage polarization, we first analyzed the correlation of ZEB1 to multiple immune cell infiltration using TIMER 2.0. The results showed that ZEB1 was significantly correlated with the infiltration of these six types of immune cells. Among them, it has the strongest correlation with macrophage infiltration (Figure S4). Further, we constructed ZEB1 low expressing NPC cell lines (Figure S5A). We treated macrophages with conditioned media of different group of 5–8F and 6–10B cells. Further, we determined the changes in macrophage polarization by detecting the differences in the expression of M1 and M2 macrophage markers in different groups of macrophages. The results of qRT-PCR showed that the expression of M2 macrophage markers (IL-10, CD163 and CD206) was reduced in macrophages treated with si-ZEB1 NPC cell CM (Figure 8A, all $P < 0.05$). Inhibition of ZEB1 expression in CM of NPC cells had no effect on the transcription level of M1 macrophage markers (IL-6, TNF-α and CD80) (Figure 8A). The results of ELISA assay also showed that down-regulating the expression of ZEB1 in 5–8F and 6–10B cells did not affect the level of TNF-α in macrophages, but significantly reduced the expression level of IL-10 (Figure 8B, $P < 0.01$). All the above results showed that inhibition of ZEB1 expression only down-regulated the expression of M2 macrophage markers. Therefore, we further detected the expression of M2 macrophage marker protein CD206 in macrophages of each group by immunofluorescence staining. The results also showed that the expression of CD206 in macrophages of 5–8F/6-10B-si-ZEB1-CM group was significantly down-regulated (Figure 8C, all $P < 0.01$). Hence, the regulatory effect of ZEB1 on macrophages is mainly targeted at M2 macrophages. Finally, through macrophage chemotaxis experiments, we confirmed that inhibition of ZEB1 expression could alleviate the chemotaxis of M2 macrophages on cancer cells (Figure S6). Next, we verified that circ_CIT regulates M2 macrophage polarization through ZEB1. We constructed ZEB1 high expressing NPC cell lines (Figure S5B). We treated macrophages with conditioned media of different group of 5–8F and 6–10B cells. The results showed that the expression of M2 macrophage markers was reduced in macrophages treated with si-circ_CIT NPC cell CM. The addition of oe-ZEB1 reversed the above trend (Figure 9A, all $P < 0.05$). The results of ELISA assay also showed that down-regulating the expression of circ_CIT in 5–8F and 6–10B cells did not affect the level of TNF-α in macrophages, but significantly reduced the expression level of IL-10. The addition of oe-ZEB1 upregulated the expression level of IL-10 (Figure 9B, all $P < 0.05$).

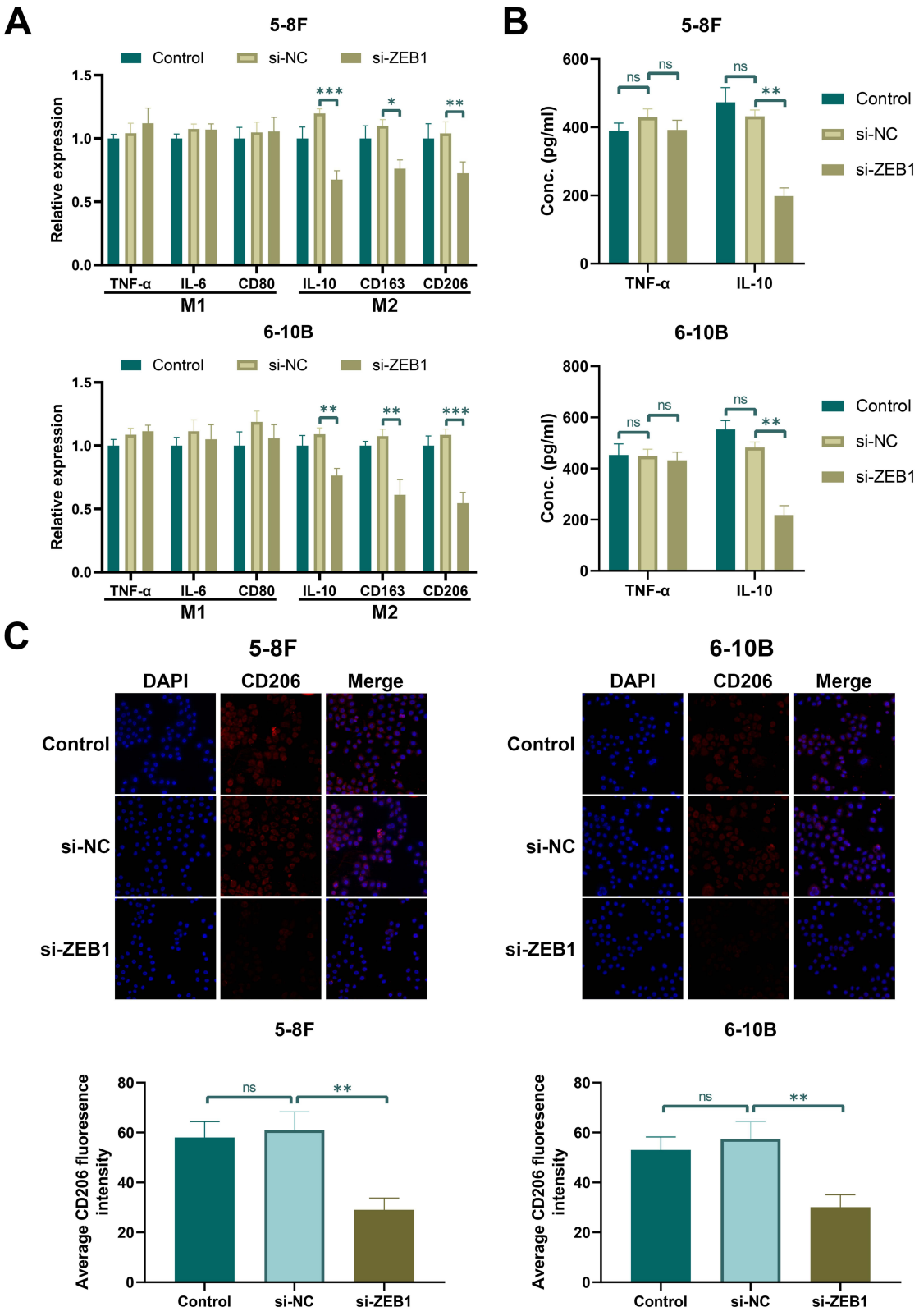

Figure 8 ZEB1 promotes M2 macrophage polarization by NPC cells. (**A**) The transcription levels of M1 macrophage markers (IL-6, TNF-α and CD80) and M2 macrophage markers (CD206, CD163 and IL-10) in macrophages treated with 5–8F or 6–10B medium of different treatment groups were detected by qRT-PCR. (**B**) The protein levels of TNF-α and IL-10 in macrophages treated with 5–8F or 6–10B medium of different treatment groups were detected by ELISA. (**C**) The expression levels of CD206 in macrophages treated with TNF-α and IL-10 medium of different treatment groups were detected by immunofluorescence staining. All n=3. ns represents no significantly difference, * $P < 0.05$, ** $P < 0.01$, *** $P < 0.001$.

https://doi.org/10.2147/CMAR.S526022

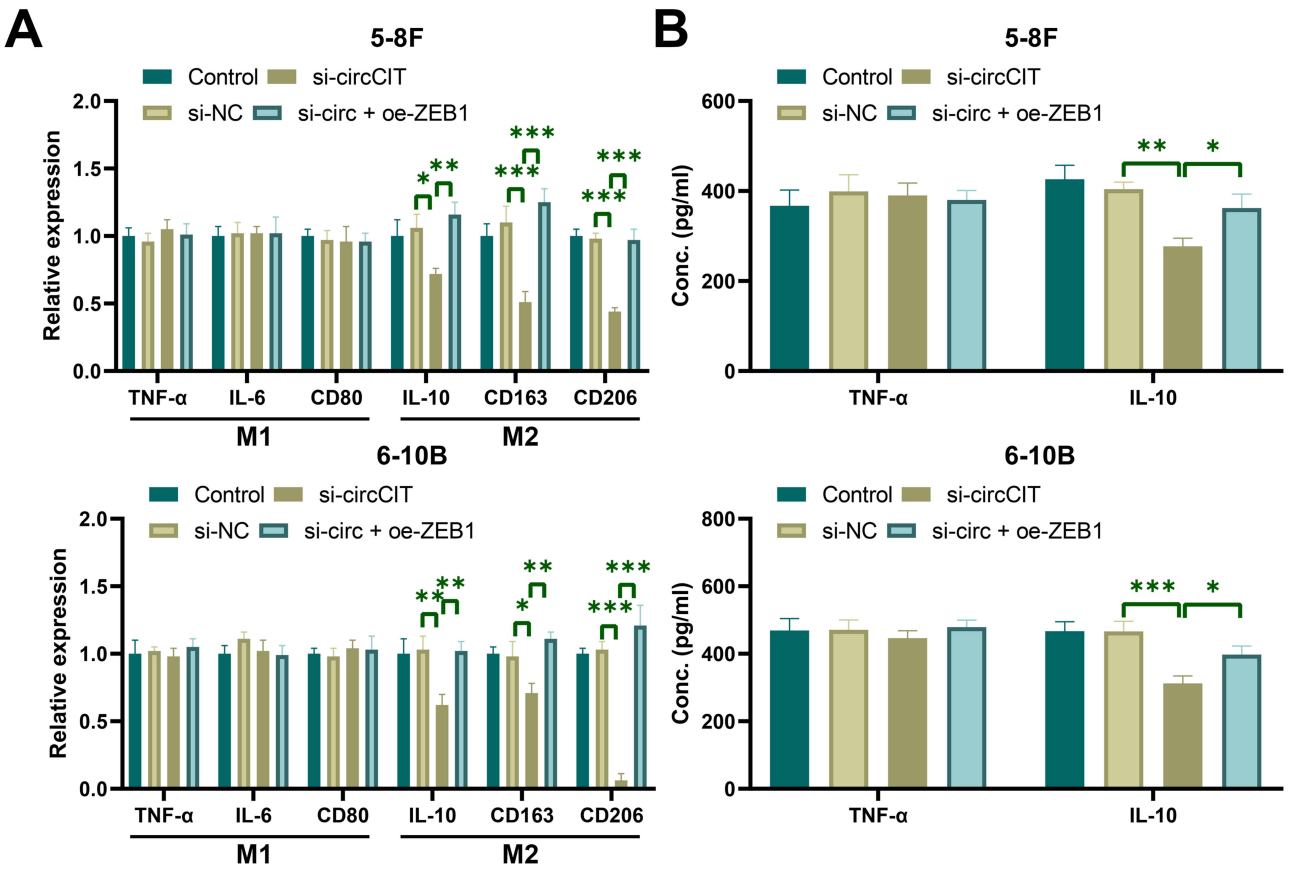

Figure 9 Circ_CIT promotes M2 macrophage polarization by NPC cells by ZEB1. (**A**) The transcription levels of M1 macrophage markers (IL-6, TNF-α and CD80) and M2 macrophage markers (CD206, CD163 and IL-10) in macrophages treated with 5–8F or 6–10B medium of different treatment groups were detected by qRT-PCR. (**B**) The protein levels of TNF-α and IL-10 in macrophages treated with 5–8F or 6–10B medium of different treatment groups were detected by ELISA. All n=3. * $P < 0.05$, ** $P < 0.01$, *** $P < 0.001$.

Discussion

It is known that circRNAs are involved in the regulation of many cellular processes and often become dysfunctional in most types of cancer.[17,18] Our research group found abnormal expression of circ_CIT in NPC tissues and cells through qRT-PCR analysis. We found that circ_CIT was highly expressed in NPC tissues and cells, and expression level was positively correlated with patient's clinical stage, which may serve as a diagnostic marker for NPC. Aiming to uncover the biological function of circ_CIT in NPC, we knocked down the expression of circ_CIT and found that it significantly inhibited cell growth, migration, EMT and metastasis in NPC. This indicated that circ_CIT might play an oncogenic role in NPC.

CircRNAs are a particular type of non-coding RNA that lack 5′-3′ ends and poly-A tail. It has characteristics of stable structure, highly conservative property and tissue-specific expression.[9,19] In the past few decades, circRNA as a transcriptional regulator of gene expression has attracted more and more attention. Many studies have reported the regulatory role of circRNA in cancer.[6,20] For example, circ_FNDC3B, circ_PDSS1 promoted cancer progression,[21,22] while circ_ITCH suppressed cancer progression through complex signaling pathway.[23] Generally, circRNA acts as a regulator of tumor gene expression, while circRNA acts as a competitive endogenous RNA (ceRNA). The ceRNA hypothesis proposes that RNAs with miRNA target sites can bind miRNAs in competition with mRNAs, forming a coregulatory posttranscriptional network. Numerous studies imply that circRNAs can act as ceRNAs to regulate miRNAs. Consequently, the imbalance of the ceRNA network may cause tumorigenesis and its development by disrupting the expression of key circRNAs.[24] Participating in specific signaling pathways through the circRNA-miRNA-mRNA axis is currently the most common regulatory mechanism.[25,26] So far, most studies on circRNA in

NPC lacked systematic experimental verification. In our study, we aimed to investigate whether circ_CIT worked by adsorbing miR-409-3p to rescue the function of ZEB1 and inhibit the progress of NPC. Through dual luciferase reporter gene detection, we determined that miR-409-3p is a new target of circ_CIT. qRT-PCR analysis also showed that the expression of miR-409-3p was negatively correlated with the expression of circ_CIT. Further cytological experiments showed that miR-409-3p inhibited the activity of circ_CIT, thereby reversing the circ_CIT-mediated promotion of NPC tumorigenesis. Therefore, we confirmed that circ_CIT could inhibit the process of NPC by adsorbing miR-409-3p and up-regulating the expression of ZEB1.

ZEB1, also called Zinc finger E-box binding homeobox 1, is located in the nucleoplasm, the nucleolus (single cell variability). ZEB1 plays a key role in many aspects, for example, it can Inhibit interleukin-2 (IL-2) gene expression. Enhancing or repressing the promoter activity of the ATP1A1 gene depending on the quantity of cDNA and on the cell type. Suppressing E-cadherin promoter and induces an epithelial-mesenchymal transition (EMT) by recruiting SMARCA4/BRG1, etc. In fact, it has been shown that ZEB1 involved in the invasion and metastasis of several cancers. For example, Wu Y. reported that lncRNA activated Akt signaling to increase ZEB1 expression, thereby promoting epithelial-mesenchymal transition and enhancing the invasiveness of OC cells.[27] Another study showed that LncRNA ZEB1-AS1 was increased in lung adenocarcinoma cell lines, LncRNA ZEB1-AS1 silencing caused inhibition of cell proliferation and introduction of apoptosis by targeting miR-409–3p/ZEB1 axis. Upregulation of ZEB1 promoted LncRNA ZEB1-AS1 transcription, forming a positive feedback loop. Restoration of ZEB1 could partially abolished the action of ZEB1-AS1 silencing on cell proliferation and apoptosis.[28] On the other hand, ZEB1 has been found to regulate macrophage activity in the microenvironment of a variety of tumor.[29,30] Therefore, this study further explored whether abnormal ZEB1 expression also mediates NPC cells to regulate macrophage activity. The results showed that NPC cells with low expression of ZEB1 inhibited M2 polarization and chemotactic activity of macrophages. Circ_CIT regulated M2 macrophage polarization by mediating ZEB1.

The present study had certain limitations that should be acknowledged. Firstly, the regulation of circ_CIT on activity of NPC cells may be produced through various pathways and mechanism. This study focused on only miR-409-3p/ZEB1, more studies are needed to find out other regulatory mechanism of circ_CIT in the future. Secondly, the conclusions reached in this study need to be validated using more types of cancer cells (such as CNE1 and CNE2 cells), and in vivo assays in the future. Thirdly, the conclusion of this study lacks bioinformatic and omics analysis. In the future, efforts should be made to strengthen the verification of this aspect. Finally, the diagnostic and prognostic value of circ_CIT for patients with NPC needs to be verified in the future by enrolling more NPC patients.

Conclusion

In conclusion, we identified a new circRNA, circ_CIT in NPC and demonstrated that circ_CIT is overexpressed in NPC cells and tissues, which is closely associated with the progression in NPC patients. Furthermore, mechanistic research revealed that circ_CIT may adsorb miRNA to exert a tumor promotion effect, thereby enhancing the growth and invasion of NPC cells and activating the activity of tumor-associated macrophages. Our newly discovered circ_CIT/miR-409-3p/ZEB1 axis will provide new ideas for therapeutic targets in clinical cancer treatment.

Data Sharing Statement

All the results are presented in the article/supplementary material. Further inquiries can be directed to the corresponding authors.

Ethics Statement

The studies involving humans were approved by the Ethics Committee of Jiangsu Cancer Hospital (Ethics Approval Number: (2021)413). The studies were conducted in accordance with the local legislation and institutional requirements. The participants provided their written informed consent to participate in this study.

Funding

This work was supported in part by a National Natural Science Foundation of China grant (Grant number: 82003223, 82460571 and 82102850), in part by a grant from Natural Science Foundation of Guangxi, China (Grant number: 2024GXNSFAA010038), in part by China Postdoctoral Science Foundation (Grant number: 2020M671398), in part by Science and Technology Development Fund of Nanjing Medical University (Grant number:NMUB20220157).

Disclosure

The authors report no conflicts of interest in this work.

References

1. Luo W. Nasopharyngeal carcinoma ecology theory: cancer as multidimensional spatiotemporal "unity of ecology and evolution" pathological ecosystem. *Theranostics*. 2023;13(5):1607–1631. doi:10.7150/thno.82690
2. Hsieh HT, Zhang XY, Wang Y, Cheng XQ. Biomarkers for nasopharyngeal carcinoma. *Clinica Chimica Acta; International journal of Clinical Chemistry*. 2025;572:120257.
3. Zhang B, Li J, Wang Y, et al. Deubiquitinase USP7 stabilizes KDM5B and promotes tumor progression and cisplatin resistance in nasopharyngeal carcinoma through the ZBTB16/TOP2A axis. *Cell Death and Differentiation*. 2024;31(3):309–321. doi:10.1038/s41418-024-01257-x
4. Nappi F. Non-Coding RNA-Targeted Therapy: a State-of-the-Art Review. *International Journal of Molecular Sciences*. 2024;25(7):3630. doi:10.3390/ijms25073630
5. Binder AK, Bremm F, Dörrie J, Schaft N. Non-Coding RNA in Tumor Cells and Tumor-Associated Myeloid Cells-Function and Therapeutic Potential. *International Journal of Molecular Sciences*. 2024;25(13):7275. doi:10.3390/ijms25137275
6. Nemeth K, Bayraktar R, Ferracin M, Calin GA. Non-coding RNAs in disease: from mechanisms to therapeutics. *Nature Reviews Genetics*. 2024;25(3):211–232. doi:10.1038/s41576-023-00662-1
7. Bonnet C, Dian AL, Espie-Caullet T, et al. Post-transcriptional gene regulation: from mechanisms to RNA chemistry and therapeutics. *Bulletin du Cancer*. 2024;111(7–8):782–790. doi:10.1016/j.bulcan.2024.04.005
8. He M, Pan Y, You C, Gao H. CircRNAs in cancer therapy tolerance. *Clinica Chimica Acta; International Journal of Clinical Chemistry*. 2024;558:119684. doi:10.1016/j.cca.2024.119684
9. Liu Q, Li S. Exosomal circRNAs: novel biomarkers and therapeutic targets for urinary tumors. *Cancer Letters*. 2024;588:216759. doi:10.1016/j.canlet.2024.216759
10. Wang D, Tang L, Chen M, et al. Nanocarriers Targeting Circular RNA ADARB1 Boost Radiosensitivity of Nasopharyngeal Carcinoma through Synergically Promoting Ferroptosis. *ACS nano*. 2024;18(45):31055–31075. doi:10.1021/acsnano.4c07676
11. Peng M, Zhang S, Wu P, et al. Circular RNA circCLASP2 promotes nasopharyngeal carcinoma progression through binding to DHX9 to enhance PCMT1 translation. *Molecular Cancer*. 2025;24(1):67. doi:10.1186/s12943-025-02272-3
12. Yin L, Chen J, Ma C, et al. Hsa_circ_0046263 functions as a ceRNA to promote nasopharyngeal carcinoma progression by upregulating IGFBP3. *Cell Death & Disease*. 2020;11(7):562. doi:10.1038/s41419-020-02785-3
13. Yang Y, Hua W, Zeng M, Yu L, Zhang B, Wen L. A ceRNA network mediated by LINC00475 in papillary thyroid carcinoma. *Open Medicine (Warsaw, Poland)*. 2022;17(1):22–33. doi:10.1515/med-2021-0389
14. Peng R, Cao J, Su BB, et al. Down-regulation of circPTTG1IP induces hepatocellular carcinoma development via miR-16-5p/RNF125/JAK1 axis. *Cancer Letters*. 2022;543:215778. doi:10.1016/j.canlet.2022.215778
15. Chen Y, Wang J, Heng Y, Guo Y, Ding K, Ma C. MIR155HG promotes metastasis and cisplatin resistance of cervical cancer cells by regulating the miR-409-3p and ZEB1 axis. *Scientific Reports*. 2025;15(1):20541. doi:10.1038/s41598-025-08727-3
16. Hu R, Xu B, Ma J, et al. LINC00963 promotes the malignancy and metastasis of lung adenocarcinoma by stabilizing Zeb1 and exosomes-induced M2 macrophage polarization. *Molecular Medicine (Cambridge, Mass)*. 2023;29(1):1. doi:10.1186/s10020-022-00598-y
17. Conn VM, Chinnaiyan AM, Conn SJ. Circular RNA in cancer. *Nature Reviews Cancer*. 2024;24(9):597–613. doi:10.1038/s41568-024-00721-7
18. Li Z, Yin S, Yang K, et al. CircRNA Regulation of T Cells in Cancer: unraveling Potential Targets. *International Journal of Molecular Sciences*. 2024;25(12):1.
19. Yi Q, Feng J, Lan W, Shi H, Sun W. CircRNA and lncRNA-encoded peptide in diseases, an update review. *Molecular Cancer*. 2024;23(1):214. doi:10.1186/s12943-024-02131-7
20. Qiu M, Chen Y, Zeng C. Biological functions of circRNA in regulating the hallmarks of gastrointestinal cancer (Review). *International Journal of Oncology*. 2024;64(5). doi:10.3892/ijo.2024.5637
21. Luo G, Li R, Li Z. CircRNA circFNDC3B promotes esophageal cancer progression via cell proliferation, apoptosis, and migration regulation. *Int J Clin Exp Pathol*. 2018;11(8):4188–4196.
22. Ouyang Y, Li Y, Huang Y, et al. CircRNA circPDSS1 promotes the gastric cancer progression by sponging miR-186-5p and modulating NEK2. *Journal of Cellular Physiology*. 2019;234(7):10458–10469. doi:10.1002/jcp.27714
23. Wang M, Chen B, Ru Z, Cong L. CircRNA circ-ITCH suppresses papillary thyroid cancer progression through miR-22-3p/CBL/beta-catenin pathway. *Biochemical and Biophysical Research Communications*. 2018;504(1):283–288.
24. Zhang C, Yu Z, Yang S, et al. ZNF460-mediated circRPPH1 promotes TNBC progression through ITGA5-induced FAK/PI3K/AKT activation in a ceRNA manner. *Molecular Cancer*. 2024;23(1):33.
25. Firoozi Z, Shahi A, Mohammadisoleimani E, et al. CircRNA-associated ceRNA networks (circCeNETs) in chronic obstructive pulmonary disease (COPD). *Life Sciences*. 2024;349:122715. doi:10.1016/j.lfs.2024.122715
26. Kohansal M, Alghanimi YK, Banoon SR, et al. CircRNA-associated ceRNA regulatory networks as emerging mechanisms governing the development and biophysiopathology of epilepsy. *CNS Neuroscience & Therapeutics*. 2024;30(4):e14735. doi:10.1111/cns.14735

27. Wu Y, Zhu B, Yan Y, et al. Long non-coding RNA SNHG1 stimulates ovarian cancer progression by modulating expression of miR-454 and ZEB1. *Molecular Oncology*. 2021;15:1584–1596. doi:10.1002/1878-0261.12932
28. Qu R, Chen X, Zhang C. LncRNA ZEB1-AS1/miR-409-3p/ZEB1 feedback loop is involved in the progression of non-small cell lung cancer. *Biochemical and Biophysical Research Communications*. 2018;507(1–4):450–456. doi:10.1016/j.bbrc.2018.11.059
29. Chen XJ, Guo CH, Wang ZC, et al. Hypoxia-induced ZEB1 promotes cervical cancer immune evasion by strengthening the CD47-SIRPα axis. *Cell Communication and Signaling: CCS*. 2024;22(1):15. doi:10.1186/s12964-023-01450-4
30. Ou Y, Jiang HM, Wang YJ, et al. The Zeb1-Cxcl1 axis impairs the antitumor immune response by inducing M2 macrophage polarization in breast cancer. *American journal of Cancer Research*. 2024;14(9):4378–4397. doi:10.62347/UAIS7070